

# Carbon “Onions” as Point Electron Sources

Ming-Sheng Wang,\* Dmitri Golberg,\* and Yoshio Bando

International Centre for Materials Nanoarchitectonics (MANA), National Institute for Materials Science (NIMS), Namiki 1-1, Tsukuba, Ibaraki 3050044, Japan

**ABSTRACT** The novel type of an electron field emitter is demonstrated by welding a single carbon “onion” onto the end of a tungsten tip inside a high-resolution transmission electron microscope. Such merged structure is found to markedly reduce the onset voltage peculiar to a standard tungsten field emitter due to the small size of the onion and its highly curved surface. Similar to short carbon nanotubes, individual C-onion emitters can sustain large emission currents, more than 100  $\mu\text{A}$ , and exhibit good long-term emission stability. Moreover the insertion of a high electrical resistance in series can suppress the current fluctuation to only 1.9%. All these properties make these newly created field emitters promising candidates for the advanced point electron sources.

**KEYWORDS:** carbon onion · field emission · point electron sources · tungsten tip · TEM-STM · carbon nanotube

Carbon nanotube (CNT) electron sources have a high potential for commercial applications such as field emission (FE) displays and high-resolution electron-beam instruments.<sup>1–4</sup> Most advantages of a CNT emitter come from its specifically closed atomic cap which is distinctive from those of the commonly used emitters such as tungsten. The CNT caps usually have a small diameter of a few to tens nanometers. Each carbon atom within the cap is bound to three other carbon atoms by strong covalent  $\text{sp}^2$  bonds. Such CNT ends can lead to a low operation voltage and, more importantly, good FE stability. That is because the activation energy for surface migration of C atoms is much larger than that for a tungsten electron source. This allows the CNT cap to withstand the extremely strong fields, up to  $\sim 10$  V/nm.<sup>5,6</sup> Besides, carbon has one of the lowest sputtering coefficients, which favorably allows an electron source to resist the bombardment of positive ions.<sup>7</sup> As a result, the CNT cap is actually the crucial part of a whole nanotube, since the majority of electrons is extracted from the apex where the electrical field is concentrated.

The CNT shank, by contrast, plays a less important role, although a long shank can increase the aspect ratio, and therefore, improve the field enhancement factor and reduce the applied voltage needed for field emission. In a FE operation, a long tube may eventually lead to poor emission stability and even structural damage due to Joule heating,<sup>3,8–12</sup> because the temperature increase induced by resistive heating depends strongly on the square of structure length.<sup>13,14</sup> Especially, when individual CNTs are used as point electron sources in high-resolution imaging apparatuses, the thermal vibration amplitude of the tube end will significantly increase with the tube length, thus reducing the image resolution.<sup>15</sup> Therefore, engineers prefer short nanotubes (tens to a few hundreds nanometers) as the point electron emitters.<sup>1,2,5</sup>

The extreme case of a shortened capped multiwalled CNT is a carbon onion. In this work, we demonstrate a novel prototype electron point source emitter made of a single C “onion” as the cap and a tungsten tip as the shank. These two parts are firmly connected through an intermediate carbide layer using an *in situ* Joule-heating process inside a high-resolution transmission electron microscope (HRTEM) equipped with a scanning tunneling microscope (STM) unit. The C onion dramatically lowers the FE onset voltage of the tungsten tip emitter and shows fairly good emission stability and high FE current which rival a short CNT emitter.

## RESULTS AND DISCUSSION

The fabrication and FE measurements of such C onion–tungsten structures were carried out inside a high-resolution JEM-3100FEF (JEOL, Omega Filter) transmission

\*Address correspondence to  
WANG.Mingsheng@nims.go.jp,  
GOLBERG.Dmitri@nims.go.jp.

Received for review June 14, 2010  
and accepted July 12, 2010.

Published online July 20, 2010.  
10.1021/nn1013353

© 2010 American Chemical Society

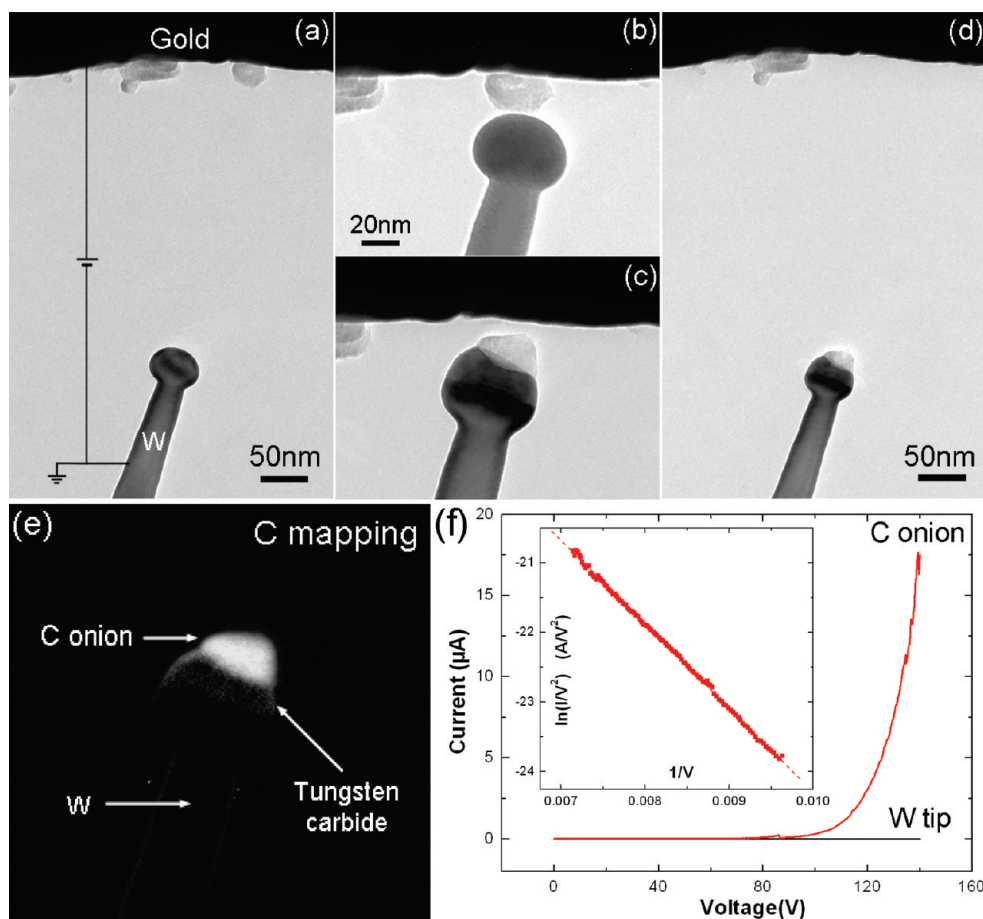


**Figure 1.** (a) TEM image showing the field emission measurement on a standard W tip. This tip was then moved to contact a C onion attached to the counter gold wire (b), the tip and onion were then fused together at a high current (c). (d) The newly formed C-onion/W-tip structure was retracted to the original position as in image a for a comparative FE measurement. (e) EELS C map showing the spatially resolved carbon distribution within the emitter end in image d. (f) The measured FE  $I$ – $V$  curves and  $F$ – $N$  plot corresponding to the  $I$ – $V$  curve recorded from the C-onion emitter (inset).

electron microscope (TEM) equipped with a piezo-driven STM holder.<sup>16</sup> As shown in Figure 1a, a W tip obtained by electrochemical etching was moved to face a gold wire. The tip-end has intentionally been pre-melted into a ball-like shape to remove the contamination and improve its conductance. A voltage sweep up to 140 V was applied onto the gold anode; however, no FE current from the W tip was detected (the black  $I$ – $V$  curve in Figure 1f). This W tip was then moved to touch a carbon onion that was preattached to the edge of the gold wire (Figure 1b). A constant voltage of 1 V was applied to the gold wire with a current limit of less than 1  $\mu$ A. At the moment when the current limit was switched to 1 mA, half of the C onion was suddenly attached to the W end. Such fusion reaction occurred due to the abruptly increased current and corresponding Joule heating effect, and halted immediately once the C onion detached from the gold wire (Figure 1c). As a result, the top half of the onion was still exposed upon the W tip. Then the W tip was retracted to its original position (as shown in Figure 1a) for the second FE measurement (Figure 1d). In contrast, this newly formed C onion–W tip emitter exhibited greatly enhanced FE

and a low onset voltage (here we use 1 nA as the reference for the onset voltage) of only  $\sim 70$  V (the red  $I$ – $V$  curve in Figure 1f). This can be mainly attributed to the fact that C onions usually show an irregular polyhedron-like shape (for more samples see, *e.g.*, Figures 2a and 4b), and some local surface sites are extremely curved. These would offer the effective emitting areas.

We use the  $F$ – $N$  equation to analyze the experimental FE  $I$ – $V$  curves, and the FE current  $I$  is given by<sup>17,18</sup>

$$I = A(1.54 \times 10^{-6}/\phi t(y)^2)F^2 \exp(-6.83 \times 10^9 \phi^{3/2} v(y)/F) \quad (1)$$

where  $A$  is the emitting area, and  $\phi$  is the work function. The functions  $t(y)$  and  $v(y)$  can be approximated well by  $t(y) = 1 + 0.1107y^{1.33}$  and  $v(y) = 1 - y^{1.69}$ , where  $y = 3.79 \times 10^{-5} F^{1/2}/\phi$ .<sup>9,18</sup> The local electric field  $F$  is related to the applied voltage  $V$  via  $F = \beta V$ , with  $\beta$  being the field conversion factor.  $FN$  plots were obtained from  $I$ – $V$  curves via plotting  $\ln(I/V^2)$  vs  $1/V$ . As shown in the inset of Figure 1f, the  $F$ – $N$  plot approaches a straight line, suggesting metallic FE behavior of the C onion. We then calcu-

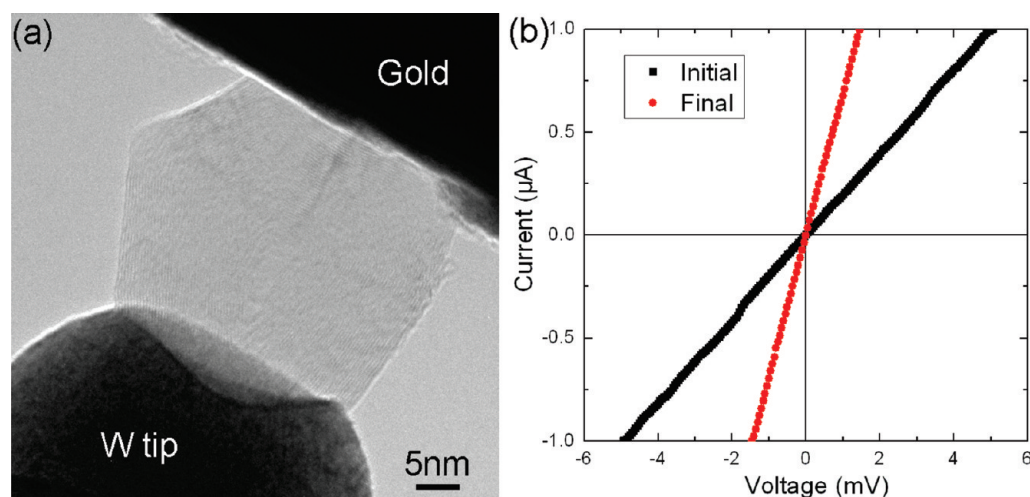


Figure 2. (a) Two-terminal electrical measurements of the C-onion/W-tip junction by contacting the C onion with the gold electrode. (b) The corresponding  $I$ – $V$  curves obtained in a low bias region and showing a decreased resistance, from 5 to 1.4 k $\Omega$ , due to compression of the C onion toward the gold contact and the onion deformation.

lated the emitting area  $A$  by fitting the  $FN$  plot and using the work function  $\phi = 5$  eV, as for closed CNT<sup>2</sup> (see ref 9 for calculation details). The obtained  $A$  is 69 nm<sup>2</sup>, much smaller than the surface area of the C-onion that has a diameter of 32 nm. This confirms that the effective emitting area has originated from the local area of the onion surface with a small radius of curvature. We also notice that this new emitter can sustain a FE current of at least 17  $\mu$ A (see Figure 1f), and the  $F$ – $N$  plot still remains linear even under such high current. By contrast, previous studies have documented that a FE current of only  $\sim 1$   $\mu$ A can heat a 40  $\mu$ m-long CNT to 2000 K at the apex, which results in a considerable deviation of  $F$ – $N$  plot from the linear behavior due to thermally enhanced emission.<sup>13</sup> These results clearly show the importance of the shortened length that can effectively suppress the Joule heating effect of the CNT emitter. This is also the prime advantage of the fabricated novel emitter.

In addition, as revealed by elemental mapping of the whole W tip-end using spatially resolved electron energy loss spectroscopy (EELS), the lower half of the C onion is found to be already dissolved into the head of the W tip to form a layer with a weak bright contrast on the C map (Figure 1e). Such layer has been confirmed to be tungsten carbide (WC) in our previous detailed studies of the CNT/W junctions.<sup>16</sup> Formation of tungsten carbide layer indicates a strong coupling between C onion and W tip. In fact, we found that it had almost been impossible to separate the C onion from the W tip by simply scratching or bending such junctions on a gold surface. The strong connection could also be confirmed by putting such structure under extremely high positive field for 20 min.<sup>6</sup> The latter only caused the local evaporation of the onion without any sign

of its separation from the W tip (see Supporting Information, Figure S1).

We also tested the electrical properties of such structures *via* two-terminal measurements by contacting the C onion to a gold wire (Figure 2a). The obtained  $I$ – $V$  curve indicates a good Ohmic conduction of the whole system with a resistance of 5 k $\Omega$  (black line in Figure 2b). In addition, the resistance can further be reduced when we squeeze the C onion by pushing the W tip toward gold wire until the recorded  $I$ – $V$  curve stops changing (red line in Figure 2b). The improvement of the conduction might arise from the enhanced interlayer electron transport within the C onion under compression or increased contact area between the onion and gold electrode. The final very low resistance of 1.4 k $\Omega$  confirms the excellent electrical contact between W and C-onion, as well as the good conduction of the tungsten carbide layer, as expected.

As-fabricated C-onion emitters showing excellent mechanical and electrical connection with the supporting W tips therefore possess a rich potential for practical point electron sources, especially in a high applied field and FE current range. We then explored the maximum FE current ( $I_{\max}$ ) that could be extracted from such an emitter. Figure 3a shows a representative experimental run, in which a C-onion emitter was placed at a distance of 300 nm from the counter gold wire. The HRTEM image in Figure 3b presents a nearly spherical onion whose lower part has been absorbed and converted into tungsten carbide (see Supporting Information Movie S1 for the *in situ* TEM fabrication process). The voltage sweeps with an increased range (in steps of 10 V) were successively applied to the gold anode to push the C-onion to its FE current limit.<sup>5</sup> Finally, the emitter failed at a current of 122  $\mu$ A. The  $I$ – $V$  curve causing the FE failure is depicted in Figure 3d. From the

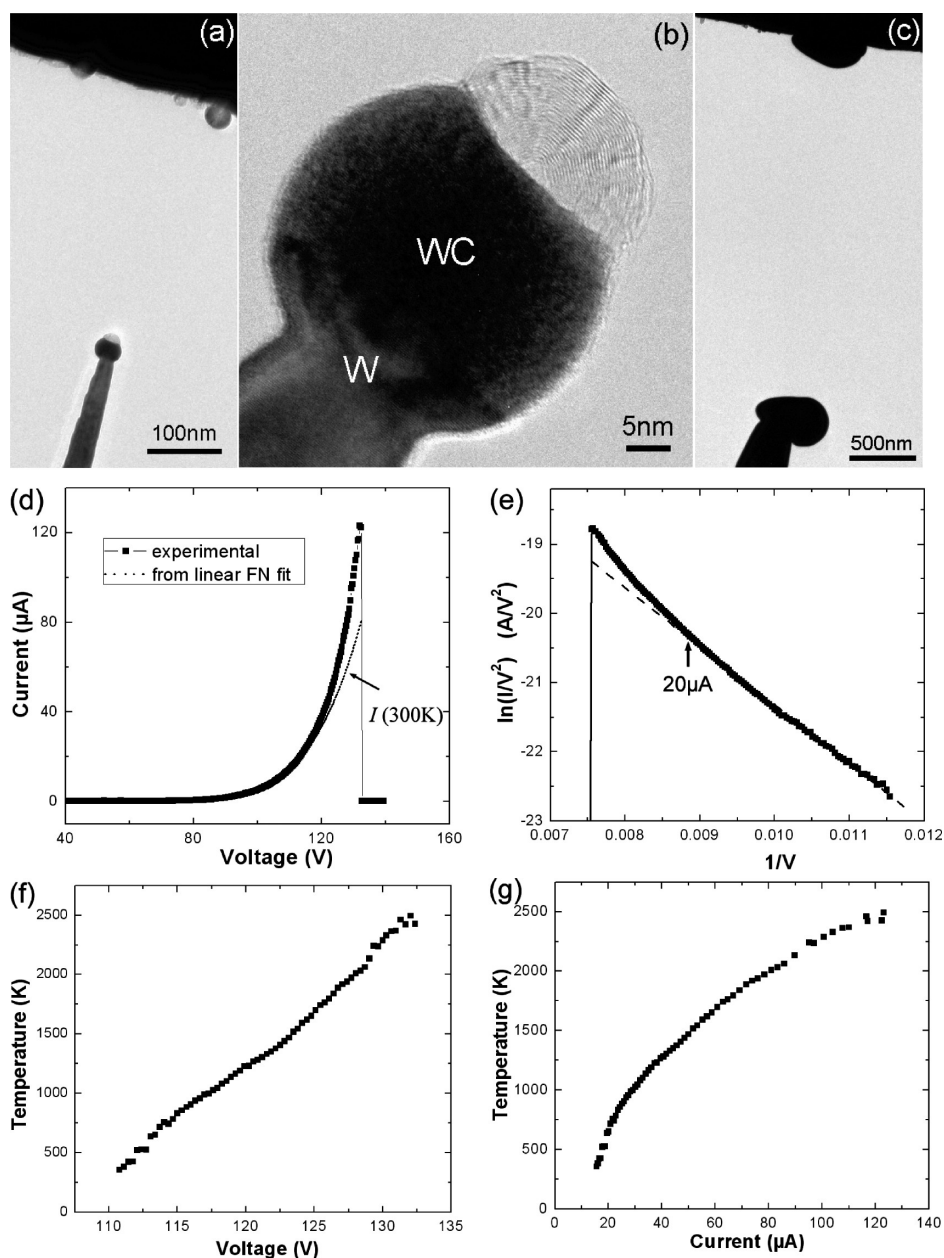


**Figure 3.** A C-onion emitter prepared for the FE measurement (a) and the corresponding HRTEM image of the emitter end (b). The final structure of the emitter destroyed due to an arcing event at a high FE current (c). The corresponding  $I$ – $V$  curve (d) and  $F$ – $N$  plot (e) obtained from the last voltage sweep causing FE failure. The dashed lines indicate the linear fitting of  $F$ – $N$  plot at the low voltage range (e) and the corresponding extrapolated  $I$ – $V$  curve (d), respectively. The calculated temperature as a function of voltage, (f) and current (g), *i.e.*,  $T$ – $V$  and  $T$ – $I$  curves, respectively.

corresponding  $F$ – $N$  plot (Figure 3e) one can see an obvious nonlinear character in a high voltage regime due to the enhanced thermionic emission. The point where the  $F$ – $N$  plot starts to deviate from the linear behavior (indicated by an arrow in Figure 3e) corresponds to a current of around 20  $\mu\text{A}$ , and the Joule heating effect below this current is expected to be negligible. We therefore estimate the field conversion factor to be  $1/12.4 \text{ nm}^{-1}$  by linear fitting the  $F$ – $N$  plot within such low current region (the dashed line in Figure 3e). Since the emitter failed at a voltage of 132 V, the maximum local field ( $F = \beta V$ ) is calculated to be 10.6 V/nm, which is consistent

with the best pre-existing short-CNT emitters (9–11 V/nm).<sup>5</sup>

Since total emission current  $I$  is contributed from both “pure” field and thermally assisted emission, we define the former part as  $I_F$  (0 K). The relationship between  $I$  and  $I_F$  can be described as<sup>19,20</sup>

$$I(V, T) = I_F(V, 0 \text{ K}) \frac{\pi k_B T / d}{\sin(\pi k_B T / d)} \quad (2)$$

where

$$d = \frac{heF}{4\pi\sqrt{2m\phi t(y)}}$$

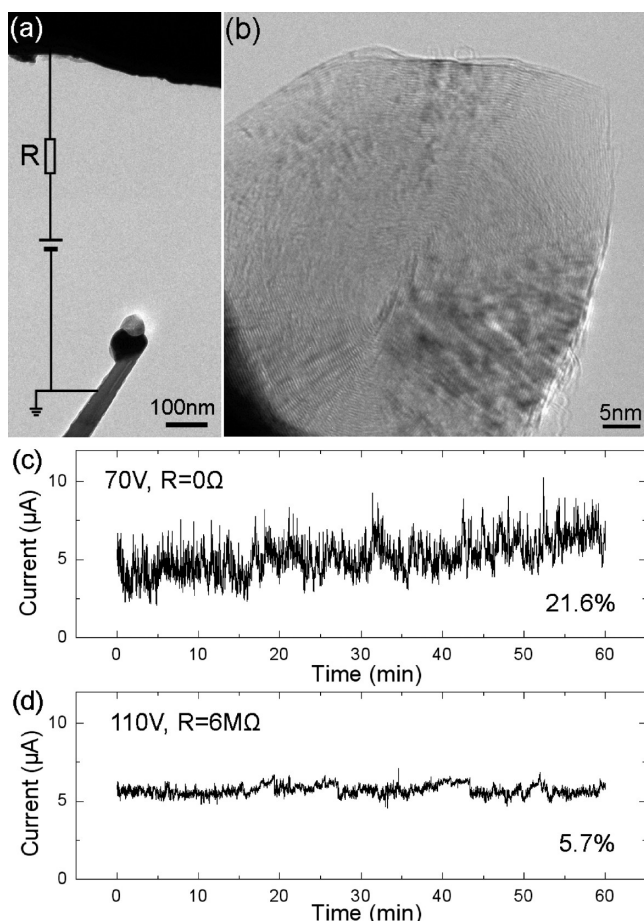


**Figure 4.** Long-term emission stability measurements on a C-onion emitter (a) and the corresponding HRTEM image of the emitter-tip end structure (b). FE current as a function of time over a 1-h continuous operation at a constant voltage (c) without and (d) with the insertion of a resistance of 6 M $\Omega$  in series.

(Strictly speaking, the complete expression in the integral form should be used instead of the eq 2 for a very high temperature.<sup>19,20</sup> However, herein for simplicity we just use eq 2 to get a rough estimation of the temperatures) In general, the higher the temperature, the larger is the ratio  $I/I_F$ . The dashed line in Figure 3d indicates the current extrapolated from the  $F-N$  fit of low voltage/current data (*i.e.*, the dashed line in Figure 3e). It is worth noting, however, that even such fitting current cannot be attributed to “pure” field emission, since the C-onion emitter is assumed to be at room temperature in the low current range. Therefore, the extrapolated current in Figure 3d is more precisely defined as  $I(300\text{ K})$ , though its difference from  $I_F(0\text{ K})$  is usually negligible (especially at a high field). Similarly, the relationship between  $I$  and  $I(300\text{ K})$  can be further given by the equation

$$I(V, T) = I(V, 300\text{ K}) \frac{\sin(300\pi k_B/d) \times T}{\sin(\pi k_B T/d) \times 300\text{ K}} \quad (3)$$

The temperature  $T$  of the C-onion cap can be obtained by numerically solving eq 3 for any given  $V$  (or  $d$ ). Figure 3 panels f and g, respectively, show the  $T-V$  and

$T-I$  curves that are calculated from the  $I-V$  curves in Figure 3d. It is seen in Figure 3g that at the current of  $\sim 20\ \mu\text{A}$ , the heating effect becomes obvious and the corresponding temperature increases to 500 K. The temperature continues to increase to 2000 K at a current of  $\sim 80\ \mu\text{A}$ , and finally results in the FE failure at 2500 K.

Other probed C-onion emitters can typically sustain a current of 40–100  $\mu\text{A}$  (see Supporting Information, Table S1 and Figure S2), which is comparable to short-CNT emitters.<sup>5,21,22</sup> A variety of  $I_{\text{max}}$  arises from several factors such as the diameter of a C-onion and W-tip end, their contact area, and the anode–cathode distance. Especially for the latter, in order to get a high current during FE measurements, we had to place the emitter very close to the gold wire ( $<1\ \mu\text{m}$ ) because of the limitation of the maximum applied voltage (140 V) in our measurement setup. This, however, might easily cause a catastrophic arcing event at a high FE current resulting in melting/deterioration of the emitter. It is well-known that carbon, tungsten, and tungsten carbide all have very high melting points of more than 3000 K. In our FE measurements, the calculated maximum temperature before FE failure was always below these melting points, indicating that the failure was not due to the sole Joule heating effect. The most probable reason we may propose here is the thermally assisted field evaporation of the C-onion emitter that creates a conduction channel between the two electrodes, leading to an abrupt discharge. Consequently, a part of the W tip was melted/dissipated and deposited as a droplet at the edge of the counter gold wire under the attraction owing to a high electric field (see Figure 3c). Actually, nearly all presently tested C-onion emitters finally failed in line with such a mechanism. We believe that the C-onion emitters should sustain even larger FE currents if arcing can be prevented by putting the emitters far away from an anode at a higher extracted voltage.

Finally we studied the long-term FE stability of the new emitters. As displayed in Figure 4a, a C-onion emitter was placed 500 nm away from the gold anode. This C-onion contained a sharp corner served as the apex of the whole emitter (Figure 4b). Continuous measuring of the FE current was first carried out at a constant voltage of 70 V over 1 h (Figure 4c). To analyze the data points and evaluate the current stability, we use the following definition: fluctuation = (standard deviation values)/(mean values).<sup>3</sup> The fluctuation in Figure 4c is found to be 21.6%, which is mainly caused by the adsorbates inevitable at the present TEM vacuum level of  $10^{-5}$  Pa. To further stabilize the FE current, we inserted a 6 M $\Omega$  resistor in series (see schematic in Figure 4a) as a negative feedback system.<sup>23</sup> Meanwhile, the bias was set to 110 V to maintain the same FE current level ( $\sim 5\ \mu\text{A}$ ) as during the former measurement. As shown in Figure 4d, the current fluctuation in the next 1-h emission was dramatically reduced to 5.7%. Different from a CNT emitter, for which long-term emission might lead to dramatic destruction and shortening of the nanotube in a current range of a few  $\mu\text{A}$  or

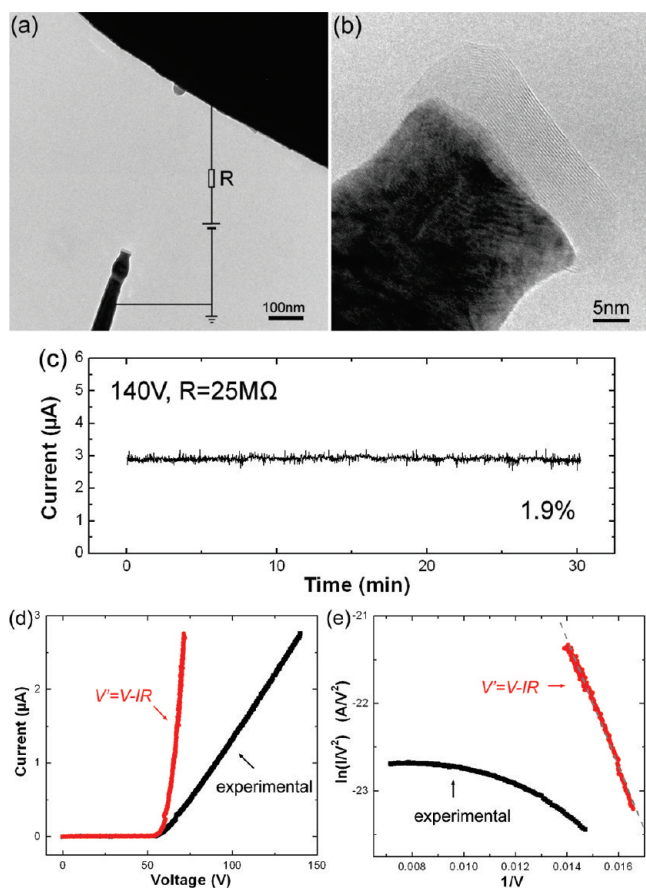


**Figure 5.** (a) TEM image showing the field emission measurement on a C-onion emitter that is connected in series with a resistance of 25 M $\Omega$ . (b) HRTEM image of the emitter-tip-end structure. (c) FE current as a function of time over a 30-min continuous operation at a constant voltage of 140 V. (d) The measured  $I$ – $V$  curve (black line) and a new  $I$ – $V'$  curve (red line) obtained by subtracting the bias on the resistor from the overall applied voltage. Their corresponding  $F$ – $N$  plots are shown in panel e.

even less,<sup>3,24</sup> no notable structural change was found by examining the final state of the C-onion after the present measurements, indicating good long-term endurance of the C-onion at a FE current of microamperes level.

The stabilization of the FE current is essential when an electron source is utilized in electron-beam-driven instruments, such as TEM, SEM, etc. It has been reported that the practical SEM operation requires a current fluctuation smaller than 3% over 5 min for the slow scanning image acquisitions.<sup>25</sup> As a matter of fact, the current stability of the present C-onion emitters can be further improved by simply increasing the circuit resistance. Figure 5 demonstrates the related example, where a much higher series resistance of 25 M $\Omega$  has been used for a current range of  $\sim 3$   $\mu$ A at a bias of 140 V. The 30-min

continuous operation of the C-onion exhibits a further suppressed current fluctuation of 1.9%. The latter already meets the basic requirements for the practical SEM operations. As a comparison, the best performance CNT emitters have shown short-term peak–peak fluctuations of smaller than 0.2%,<sup>26</sup> when the nanotubes are operated under extremely high vacuum ( $<10^{-10}$  Torr) and at a high temperature (500  $^{\circ}$ C) during the emission process to continuously keep the emitters clean. Similarly, to show the full capacity of the presently fabricated emitters, we plan to test them in a system with a better vacuum level and a heating setup in the future, and we expect that the FE stability should be further improved at such conditions.

In addition, we notice that the insertion of a high resistance also results in nearly linear  $I$ – $V$  characteristics in a high voltage regime (black line in Figure 5d), instead of the usual exponential behavior. A differential resistance of 28 M $\Omega$  is obtained for the large bias regime, which is close to the series resistance of 25 M $\Omega$ . By subtracting the bias on the resistor from the overall applied voltage, a new  $I$ – $V'$  ( $V' = V - IR$ ,  $R = 25$  M $\Omega$ ) curve is plotted in red color in Figure 5d. Accordingly, such data processing also changes the  $F$ – $N$  plot from the nonlinear to basically linear character, which finally confirms the electron tunneling effect described by the conventional  $F$ – $N$  theory (Figure 5e).

## CONCLUSIONS

To conclude, the C onion-based point source field emitters were fabricated and tested inside the transmission electron microscope. Such emitters were fabricated by fusing together a C-onion cap and a W-tip shank. They exhibited specific field emission properties, such as low turn-on voltage, large emission current, good emission endurance, and stability, that rival those of individual short carbon nanotubes. The series high resistance was found to effectively suppress the FE fluctuation and dramatically change the  $I$ – $V$  and  $F$ – $N$  characters. We propose that such novel emitters can effectively be used as the point electron sources in, for example, high-resolution electron-beam-driven apparatuses in the future.

## METHODS

Carbon onions used in this work existed among a multi-walled carbon nanotube powder that was fabricated by an

arc-discharge method. The samples were assembled onto a freshly cut gold wire (0.25 mm in diameter) before each experiment by rubbing the gold wire on the C-onion/CNT flake

surface. This gold wire was then fixed by inserting it into a tiny-diameter pipe welded to the “Nanofactory Instruments” sample holder frame. An electrochemically etched tungsten wire (0.2 mm in diameter) was inserted into the movable part of the piezo-driven STM-TEM holder. The *in situ* TEM electrical probing and manipulation were performed in a JEM-3100FEF 300 kV field-emission HRTEM (Omega Filter). The W tip was premelted into a ball-like shape by touching it to the gold wire and running a large current through the circuit. Normal imaging conditions (a beam current density of 1–2 A/cm<sup>2</sup>) were used at 300 kV during all structural observations, EELS, electrical probing, and manipulations, in order to minimize electron-beam damage. The external series resistor was introduced in the electrical circuit using a “Nanofactory Instruments” connection box. Experimental videos were obtained by recording sequential TEM images using a CCD camera with a rate of 2 frames/s.

**Acknowledgment.** The work was supported by the International Center for Materials Nanoarchitectonics (MANA) of the National Institute for Materials Science (NIMS), Tsukuba, Japan. The authors thank M. Mitome, A. Nukui, and I. Yamada of MANA-NIMS for a technical support in the course of this work.

**Supporting Information Available:** . The long-term stability of a C-onion emitter at high positive field; another typical case of the field emission failure of a C-onion emitter; a table showing the maximum FE current of five different C-onion emitters; calculation details related to the temperature estimates of the C-onion emitter at a high FE current; an *in situ* TEM video showing a fusion reaction between a C onion and the W tip. This material is available free of charge via the Internet at <http://pubs.acs.org>.

## REFERENCES AND NOTES

- De Jonge, N.; Lamy, Y.; Schoots, K.; Oosterkamp, T. H. High Brightness Electron Beam from a Multiwalled Carbon Nanotube. *Nature* **2002**, *420*, 393–395.
- De Jonge, N.; Allieux, M.; Doytcheva, M.; Kaiser, M.; Teo, K. B. K.; Lacerda, R. G.; Milne, W. I. Characterization of the Field Emission Properties of Individual Thin Carbon Nanotubes. *Appl. Phys. Lett.* **2004**, *85*, 1607–1609.
- Suga, H.; Abe, H.; Tanaka, M.; Shimizu, T.; Ohno, T.; Nishioka, Y.; Tokumoto, H. Stable Multiwalled Carbon Nanotube Electron Emitter Operating in Low Vacuum. *Surf. Interface Anal.* **2006**, *38*, 1763–1767.
- Saito, Y.; Hamaguchi, K.; Hata, K.; Uchida, K.; Tasaka, Y.; Ikazaki, F.; Yumura, M.; Kasuya, A.; Nishina, Y. Conical Beams from Open Nanotubes. *Nature* **1997**, *389*, 554–555.
- Wang, M. S.; Chen, Q.; Peng, L. M. Field-Emission Characteristics of Individual Carbon Nanotubes with a Conical Tip: The Validity of the Fowler-Nordheim Theory and Maximum Emission Current. *Small* **2008**, *4*, 1907–1912.
- Wang, M. S.; Chen, Q.; Peng, L. M. Grinding a Nanotube. *Adv. Mater.* **2008**, *20*, 724–728.
- Paulmier, T.; Balat-Pichelin, M.; Le Queau, D.; Berjoan, R.; Robert, J. F. Physico-Chemical Behavior of Carbon Materials under High Temperature and Ion Irradiation. *Appl. Surf. Sci.* **2001**, *180*, 227–245.
- Wang, Z. L.; Gao, R. P.; de Heer, W. A.; Poncharal, P. *In Situ* Imaging of Field Emission from Individual Carbon Nanotubes and Their Structural Damage. *Appl. Phys. Lett.* **2002**, *80*, 856–858.
- Wang, M. S.; Peng, L.-M.; Wang, J. Y.; Jin, C. H.; Chen, Q. Quantitative Analysis of Electron Field-Emission Characteristics of Individual Carbon Nanotubes: The Importance of the Tip Structure. *J. Chem. Phys. B* **2006**, *110*, 9397–9402.
- Bonard, J. M.; Klinke, C.; Dean, K. A.; Coll, B. F. Degradation and Failure of Carbon Nanotube Field Emitters. *Phys. Rev. B* **2003**, *67*, 115406.
- Dean, K. A.; Burgin, T. P.; Chalamala, B. R. Evaporation of Carbon Nanotubes During Electron Field Emission. *Appl. Phys. Lett.* **2001**, *79*, 1873–1875.
- Wei, W.; Liu, Y.; Wei, Y.; Jiang, K. L.; Peng, L. M.; Fan, S. S. Tip Cooling Effect and Failure Mechanism of Field-Emitting Carbon Nanotubes. *Nano Lett.* **2007**, *7*, 64–68.
- Purcell, S. T.; Vincent, P.; Journet, C.; Binh, V. T. Hot Nanotubes: Stable Heating of Individual Multiwall Carbon Nanotubes to 2000 K Induced by the Field-Emission Current. *Phys. Rev. Lett.* **2002**, *88*, 105502.
- Vincent, P.; Purcell, S. T.; Journet, C.; Binh, V. T. Modelization of Resistive Heating of Carbon Nanotubes during Field Emission. *Phys. Rev. B* **2002**, *66*, 075406.
- Treacy, M. M. J.; Ebbesen, T. W.; Gibson, J. M. Exceptionally High Young’s Modulus Observed for Individual Carbon Nanotubes. *Nature* **1996**, *381*, 678–680.
- Wang, M. S.; Golberg, D.; Bando, Y. Interface Dynamic Behavior between a Carbon Nanotube and Metal Electrode. *Adv. Mater.* **2010**, *22*, 93–98.
- Fowler, R. H.; Nordheim, L. Electron Emission in Intense Electric Fields. *Proc. R. Soc. London, Ser. A* **1928**, *119*, 173–181.
- Forbes, R. G. Field Emission: New Theory for the Derivation of Emission Area from a Fowler-Nordheim Plot. *J. Vac. Sci. Technol. B* **1999**, *17*, 526–533.
- Murphy, E. L.; Good, Jr., R. H. Thermionic Emission, Field Emission, and the Transition Region. *Phys. Rev.* **1956**, *102*, 1464–1473.
- Young, R. D. Theoretical Total-Energy Distribution of Field Emitted Electrons. *Phys. Rev.* **1959**, *113*, 110–114.
- Bonard, J. M.; Maier, F.; Stockli, T.; Chatelain, A.; de Heer, W. A.; J. P.; Salvétat, J. P.; Forro, L. Field Emission Properties of Multiwalled Carbon Nanotubes. *Ultramicroscopy* **1998**, *73*, 7–15.
- Asaka, K.; Nakahara, H.; Saito, Y. Nanowelding of a Multiwalled Carbon Nanotube to Metal Surface and Its Electron Field Emission Properties. *Appl. Phys. Lett.* **2008**, *92*, 023114.
- Heinrich, H.; Essig, M.; Geiger, J. Energy Distribution of Post-Accelerated Electrons Field-Emitted from Carbon Fibres. *Appl. Phys.* **1977**, *12*, 197–202.
- Wei, Y.; Xie, C.; Dean, K. A.; Coll, B. F. Stability of Carbon Nanotubes under Electric Field Studied by Scanning Electron Microscopy. *Appl. Phys. Lett.* **2001**, *79*, 4527–2529.
- Yamamoto, S.; Fukuhara, S.; Saito, N.; Okano, H. Stabilization of Field Emission Current. *Surf. Sci.* **1976**, *61*, 535–549.
- De Jonge, N.; Allieux, M.; Oostveen, J. T.; Teo, K. B. K.; Milne, W. I. Low Noise and Stable Emission from Carbon Nanotube Electron Sources. *Appl. Phys. Lett.* **2005**, *87*, 133118.